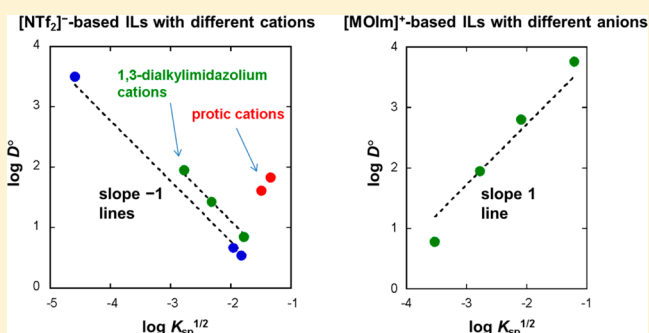


Distribution of a Monovalent Anion in Various Ionic Liquid/Water Biphase Systems: Relationship of the Distribution Ratio of Picrate Ions with the Aqueous Solubility of Ionic Liquids

Yuta Watanabe and Shoichi Katsuta*

Department of Chemistry, Graduate School of Science, Chiba University, 1-33 Yayoi-cho, Inage, Chiba 263-8522, Japan

ABSTRACT: The distribution of picrate anions in various ionic liquid (IL)/water biphase systems was investigated at 298.2 K. The ILs were 1-butyl-3-methylimidazolium hexafluorophosphate, 1-butyl-3-methylimidazolium bis(trifluoromethanesulfonyl)amide, 1-hexyl-3-methylimidazolium hexafluorophosphate, 1-hexyl-3-methylimidazolium bis(trifluoromethanesulfonyl)amide, 1-methyl-3-octylimidazolium tetrafluoroborate, 1-methyl-3-octylimidazolium hexafluorophosphate, 1-methyl-3-octylimidazolium bis(trifluoromethanesulfonyl)amide, 1-methyl-3-octylimidazolium bis(pentafluoroethanesulfonyl)amide, 1-butyl-2,3-dimethylimidazolium bis(trifluoromethanesulfonyl)amide, 1-butyl-1-methylpyrrolidinium bis(trifluoromethanesulfonyl)amide, methyltrioctylammonium bis(trifluoromethanesulfonyl)amide, 1-butylimidazolium bis(trifluoromethanesulfonyl)amide, and 1-butylpyrrolidinium bis(trifluoromethanesulfonyl)amide. The distribution ratios in dilute conditions (D°) and the aqueous solubilities of the ILs (square root of the solubility product, $K_{sp}^{1/2}$) were determined. The extractability of the picrate anion generally increases with increasing hydrophobicity of the IL cation (C^+) and increasing hydrophilicity of the IL anion (A^-). For the ILs with different C^+ but the same A^- , the $\log D^\circ$ vs $\log K_{sp}^{1/2}$ plot generally gives a linear relationship with a slope of -1 ; when the ILs have similar $K_{sp}^{1/2}$ values, the D° value decreases in the C^+ order, protic cations \gg 1,3-dialkylimidazolium cations $>$ other cations. For the ILs comprising different A^- but the same C^+ , the $\log D^\circ$ versus $\log K_{sp}^{1/2}$ plot is close to a linear line with a slope of 1. These regularities can be explained on the basis of the extraction mechanism including both the ion pair extraction with C^+ and the ion exchange with A^- .



INTRODUCTION

Liquid–liquid extraction is a simple and convenient method for recovering, removing, or concentrating organic compounds in aqueous solutions. However, the use of organic solvents which are generally volatile, flammable, and harmful has been a significant problem of this method. Recently, ionic liquids (ILs) have attracted increasing attention as replacements for conventional organic solvents because they are almost non-volatile and hence nonflammable and harmless.^{1–4} In addition, ILs have a characteristic property that they can extract ionic species without the aid of additional counterions such as ion pairing reagents.^{5–9} The mechanism of the ion extraction with ILs is generally interpreted in terms of ion exchange. For example, when the target of extraction is an anion, it is extracted from an aqueous phase to an IL phase by exchange with the component anion of the IL.^{5,6,9} On the basis of this model, the IL composed of a less hydrophobic anion is more efficient for extracting the target anion. On the other hand, the importance of hydrophobicity of the component cation of the IL is also emphasized because an imidazolium-based IL having a longer alkyl chain exhibits higher extraction ability in the anion extraction.^{8,10} There has been no quantitative explanation for such “solvent effects” of ILs on the anion extraction.

In a recent study,^{11,12} we proposed an equilibrium model including both ion pair extraction and ion exchange for the extraction of various phenolate anions with ILs. In this model, the target anion in the aqueous phase is extracted together with the IL cation in the aqueous phase and also extracted by exchange with the IL anion in the IL phase. We derived theoretical equations expressing the distribution ratio (D) of the target anion as a function of the aqueous solubility product (K_{sp}) of the IL. The dependence of D on the amount of the extracted anion was successively explained based on the equations. The dependence of D on the kind of IL was, however, not clearly explained because of not sufficient number of ILs examined.

In this study, we have investigated the distribution of picrate (2,4,6-trinitrophenolate) anions in various IL/water biphase systems for the purpose of understanding the solvent effects of ILs on the anion extraction. The reason for using picrate as the distributing anion is that this is chemically stable, is hard to be protonated, and has both high extractability and high visible-light absorption which allow us to easily measure the

Received: August 9, 2013

Accepted: February 19, 2014

Published: March 3, 2014

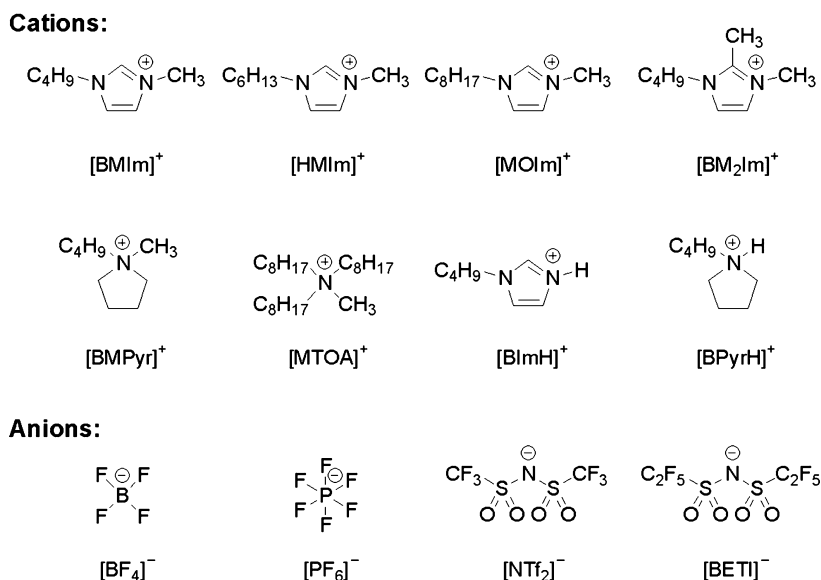


Figure 1. Structural formulas of the component ions of ILs and their abbreviations.

distribution ratio. We chose 13 kinds of hydrophobic ILs as follows: 1-butyl-3-methylimidazolium hexafluorophosphate ($[\text{BMIm}][\text{PF}_6]$), 1-butyl-3-methylimidazolium bis(trifluoromethanesulfonyl)amide ($[\text{BMIm}][\text{NTf}_2]$), 1-hexyl-3-methylimidazolium hexafluorophosphate ($[\text{HMIm}][\text{PF}_6]$), 1-hexyl-3-methylimidazolium bis(trifluoromethanesulfonyl)amide ($[\text{HMIm}][\text{NTf}_2]$), 1-methyl-3-octylimidazolium tetrafluoroborate ($[\text{MOIm}][\text{BF}_4]$), 1-methyl-3-octylimidazolium hexafluorophosphate ($[\text{MOIm}][\text{PF}_6]$), 1-methyl-3-octylimidazolium bis(trifluoromethanesulfonyl)amide ($[\text{MOIm}][\text{NTf}_2]$), 1-methyl-3-octylimidazolium bis(pentafluoroethanesulfonyl)amide ($[\text{MOIm}][\text{BETI}]$), 1-butyl-2,3-dimethylimidazolium bis(trifluoromethanesulfonyl)amide ($[\text{BM}_2\text{Im}][\text{NTf}_2]$), 1-butyl-1-methylpyrrolidinium bis(trifluoromethanesulfonyl)amide ($[\text{BMPyr}][\text{NTf}_2]$), methyltrioctylammonium bis(trifluoromethanesulfonyl)amide ($[\text{MTOA}][\text{NTf}_2]$), 1-butylimidazolium bis(trifluoromethanesulfonyl)amide ($[\text{BImH}][\text{NTf}_2]$), and 1-butylpyrrolidinium bis(trifluoromethanesulfonyl)amide ($[\text{BPyRH}][\text{NTf}_2]$). The structural formulas of the component ions are shown in Figure 1. The aqueous solubilities of the ILs were also measured to determine the K_{sp} values. The experimental data for $[\text{BMIm}][\text{PF}_6]$, $[\text{BMIm}][\text{NTf}_2]$, $[\text{MOIm}][\text{BF}_4]$, $[\text{MOIm}][\text{NTf}_2]$, and $[\text{BMPyr}][\text{NTf}_2]$ were cited from our previous paper.¹¹

EXPERIMENTAL SECTION

Materials. $[\text{HMIm}][\text{NTf}_2]$ was prepared by mixing equal volumes of aqueous solutions of $4.3 \text{ mol}\cdot\text{dm}^{-3}$ $[\text{HMIm}]\text{Cl}$ (Tokyo Chemical Industry Co., Tokyo, Japan; > 98 % purity) and $5.2 \text{ mol}\cdot\text{dm}^{-3}$ $\text{Li}[\text{NTf}_2]$ (Kanto Chemical Co., Tokyo, Japan; > 99.7 % purity). The IL phase separated from the aqueous phase was washed five times with deionized water. The yield was almost quantitative (97 %). $[\text{MOIm}][\text{BETI}]$ was prepared in a similar manner from $[\text{MOIm}]\text{Cl}$ (Wako Pure Chemical Industries, Osaka, Japan; “for organic synthesis” grade) and $\text{Li}[\text{BETI}]$ (Kishida Chemical Co., Osaka, Japan; 99 % purity) in a yield of 95 %. The purities of the products were checked by atomic absorption spectrophotometry for Li^+ and ion-selective potentiometry for Cl^- ; mass fractions $w(\text{Li}) < 4 \cdot 10^{-7}$ and $w(\text{Cl}) < 3 \cdot 10^{-6}$ for $[\text{HMIm}][\text{NTf}_2]$; $w(\text{Li}) < 3 \cdot 10^{-6}$

and $w(\text{Cl}) < 6 \cdot 10^{-6}$ for $[\text{MOIm}][\text{BETI}]$. Protic ILs, $[\text{BImH}][\text{NTf}_2]$ and $[\text{BPyRH}][\text{NTf}_2]$, were prepared as follows. 1-Butylimidazole (Sigma-Aldrich Co., St. Louis, MO; 98 % purity) or 1-butylpyrrolidine (Sigma-Aldrich Co.; 98 % purity), both of which were preliminarily purified by vacuum distillation, was added slowly to a 1.2-fold molar excess of HNTf_2 (1,1,1-trifluoro-*N*-(trifluoromethylsulfonyl)methanesulfonamide; Kanto Chemical Co.; 99.0 % purity). The mixture was washed 10 times with deionized water until the pH of the aqueous phase became a constant value (yield, > 90 %). $[\text{HMIm}][\text{PF}_6]$, $[\text{MOIm}][\text{PF}_6]$, $[\text{BM}_2\text{Im}][\text{NTf}_2]$, and $[\text{MTOA}][\text{NTf}_2]$ were the same as used previously.^{13,14} Water was distilled and further deionized with a Milli-Q Lab system (Millipore, Billerica, MA). Dichloromethane (Kanto Chemical Co.; guaranteed reagent grade) was purified by distillation. Sodium picrate monohydrate (Kanto Chemical Co.; extra-pure reagent grade) and other reagents (guaranteed reagent grade) were used as received.

Solubility Measurements. The solubilities of $[\text{HMIm}][\text{PF}_6]$, $[\text{HMIm}][\text{NTf}_2]$, $[\text{MOIm}][\text{PF}_6]$, $[\text{MOIm}][\text{BETI}]$, $[\text{BM}_2\text{Im}][\text{NTf}_2]$, $[\text{BImH}][\text{NTf}_2]$, and $[\text{BPyRH}][\text{NTf}_2]$ were determined by measuring the cation concentration in aqueous solutions saturated with the ILs at $(298.2 \pm 0.2) \text{ K}$ as follows. An aliquot of the IL-saturated aqueous solution was transferred into a stoppered glass tube, to which sodium picrate and sodium hydroxide were added so that their concentrations became $5 \cdot 10^{-2} \text{ mol}\cdot\text{dm}^{-3}$ and $1 \cdot 10^{-2} \text{ mol}\cdot\text{dm}^{-3}$, respectively; for the protic ILs, the pH of the aqueous picrate solution was adjusted to 7.0 with $1 \cdot 10^{-2} \text{ mol}\cdot\text{dm}^{-3}$ sodium dihydrogen phosphate and $6 \cdot 10^{-3} \text{ mol}\cdot\text{dm}^{-3}$ sodium hydroxide to suppress deprotonation of the protic cations. Dichloromethane, whose volume was equal to that of the aqueous solution, was further added, and the biphasic mixture was stirred for 30 min. It was preliminarily confirmed that the IL cation in the aqueous phase was quantitatively extracted into dichloromethane together with the picrate anion in a 1:1 molar ratio. The picrate concentration in the dichloromethane phase was determined spectrophotometrically ($\lambda_{\text{max}} = 367.0 \text{ nm}$, $\epsilon = 1.70 \cdot 10^4 \text{ mol}^{-1}\cdot\text{dm}^3\cdot\text{cm}^{-1}$ for $[\text{HMIm}]^+$;³ $\lambda_{\text{max}} = 367.8 \text{ nm}$, $\epsilon = 1.72 \cdot 10^4 \text{ mol}^{-1}\cdot\text{dm}^3\cdot\text{cm}^{-1}$ for $[\text{MOIm}]^+$;⁴ $\lambda_{\text{max}} = 375.0 \text{ nm}$, $\epsilon = (1.81 \pm 0.02) \cdot 10^4 \text{ mol}^{-1}\cdot\text{dm}^3\cdot\text{cm}^{-1}$ for $[\text{BM}_2\text{Im}]^+$; $\lambda_{\text{max}} = 348.6 \text{ nm}$, $\epsilon = (1.08 \pm 0.02) \cdot 10^4$

Table 1. Solubilities^a and Solubility Products of ILs in Water at 298.2 K and 0.1 MPa

No.	IL	solubility		K_{sp} (mol·dm ⁻³) ^{2b}
		mole fraction	mol·dm ⁻³	
1	[BmIm][PF ₆]	1.33·10 ^{-3c} 1.21·10 ^{-3d}	7.36·10 ^{-2c}	5.42·10 ^{-3c}
2	[BmIm][NTf ₂]	2.968·10 ^{-4c} 3.07·10 ^{-4e}	1.643·10 ^{-2c}	2.70·10 ^{-4c}
3	[HmIm][PF ₆]	4.55·10 ⁻⁴ (3·10 ⁻⁶) 4.34·10 ^{-4d}	2.52·10 ⁻² (2·10 ⁻⁴)	6.35·10 ⁻⁴
4	[HmIm][NTf ₂]	8.62·10 ⁻⁵ (3·10 ⁻⁷) 9.56·10 ^{-5e}	4.77·10 ⁻³ (2·10 ⁻⁵)	2.28·10 ⁻⁵
5	[MOIm][BF ₄]	1.1·10 ^{-3c} 1.17·10 ^{-3f}	6.2·10 ^{-2c}	3.8·10 ^{-3c}
6	[MOIm][PF ₆]	1.46·10 ⁻⁴ (1·10 ⁻⁶) 1.27·10 ^{-4d}	8.09·10 ⁻³ (7·10 ⁻⁵)	6.54·10 ⁻⁵
7	[MOIm][NTf ₂]	3.00·10 ^{-5c} 3.36·10 ^{-5e} , 2.5·10 ^{-5g}	1.66·10 ^{-3c}	2.76·10 ^{-6c}
8	[MOIm][BETI]	5.298·10 ⁻⁶ (8·10 ⁻⁹) 2.0·10 ^{-5g}	2.932·10 ⁻⁴ (4·10 ⁻⁷)	8.60·10 ⁻⁸
9	[BM ₂ Im][NTf ₂]	1.987·10 ⁻⁴ (8·10 ⁻⁷)	1.100·10 ⁻² (4·10 ⁻⁵)	1.21·10 ⁻⁴
10	[BMPyr][NTf ₂]	2.69·10 ^{-4c} 2.57·10 ^{-4h}	1.49·10 ^{-2c}	2.22·10 ^{-4c}
11	[MTOA][NTf ₂]	4.63·10 ⁻⁷ⁱ	2.56·10 ⁻⁵ⁱ	6.55·10 ⁻¹⁰
12	[BImH][NTf ₂]	8.159·10 ⁻⁴ (6·10 ⁻⁷)	4.519·10 ⁻² (3·10 ⁻⁵)	2.04·10 ⁻³
13	[BPyH][NTf ₂]	5.74·10 ⁻⁴ (2·10 ⁻⁶)	3.18·10 ⁻² (1·10 ⁻⁴)	1.01·10 ⁻³

^aValues in parentheses are standard uncertainties. ^bCalculated as the square of solubility. ^cReference 11. ^dReference 15. ^eReference 16. ^fReference 17 (295 K). ^gReference 18. ^hReference 19 (295 K). ⁱReference 14.

mol⁻¹·dm³·cm⁻¹ for [BImH]⁺; $\lambda_{max} = 350.8$ nm, $\epsilon = (1.601 \pm 0.006) \cdot 10^4$ mol⁻¹·dm³·cm⁻¹ for [BPyH]⁺). The solubility values together with the literature values^{11,14–19} are summarized in Table 1.

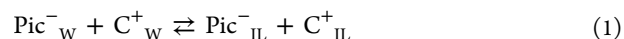
Partition Experiments. An aqueous solution of sodium picrate, whose concentration was (2.7·10⁻⁶ to 9.8·10⁻²) mol·dm⁻³, was placed in a stoppered glass tube, together with a water-saturated IL. Here, the volume of the viscous IL phase was accurately evaluated from the mass by using the densities of the ILs: 1.2937 g·cm⁻³ for [HmIm][PF₆] (dry),²⁰ 1.370 g·cm⁻³ for [HmIm][NTf₂] (dry),²¹ (1.2323 ± 0.0001) g·cm⁻³ for [MOIm][PF₆] (wet), (1.3966 ± 0.0002) g·cm⁻³ for [MOIm]-[BETI] (wet), 1.4159 g·cm⁻³ for [BM₂Im][NTf₂] (wet), 1.1113 g·cm⁻³ for [MTOA][NTf₂] (wet),¹⁴ (1.4322 ± 0.0002) g·cm⁻³ for [BImH][NTf₂] (wet), and (1.3826 ± 0.0001) g·cm⁻³ for [BPyH][NTf₂] (wet); the densities of water-saturated [MOIm][PF₆], [MOIm][BETI], [BM₂Im]-[NTf₂], [BImH][NTf₂], and [BPyH][NTf₂] were determined in this study by triplicate measurements for each IL at (298.2 ± 0.2) K with a DMA35n oscillating U-tube density meter (Anton Paar, Graz, Austria) calibrated with pure water. The volume ratio of the IL phase to the aqueous phase was adjusted to 1/10, where the volume change of the IL phase upon its dissolution into the aqueous phase was considered based on the solubility data (Table 1). The biphasic mixture in the glass tube was equilibrated by stirring with a magnetic stirrer for 1 h in a water bath thermostatted at (298.2 ± 0.2) K. After phase separation by centrifugation, the glass tube was allowed to stand for 15 min more in the thermostatted water bath. The picrate concentration in the aqueous phase ([Pic⁻]_W) was determined spectrophotometrically ($\lambda_{max} = 356.0$ nm, $\epsilon = 1.45 \cdot 10^4$ cm⁻¹·mol⁻¹·dm³). The picrate concentration in the IL phase ([Pic⁻]_{IL}) was calculated from [Pic⁻]_W and the initial aqueous concentration of sodium picrate ([Pic⁻]_{W,init}) based on the

mass balance. The distribution ratio was calculated as $D = [\text{Pic}^-]_{\text{IL}}/[\text{Pic}^-]_{\text{W}}$. The [Pic⁻]_W and log D values obtained at different [Pic⁻]_{W,init} conditions are listed in Table 2. The extraction of Na⁺ was confirmed to be negligibly small by using atomic absorption spectrophotometry.

RESULTS AND DISCUSSION

Based on the theory previously reported,¹¹ the following equilibria can be considered regarding the extraction of picrate anion (Pic⁻) from the aqueous phase to the IL phase.

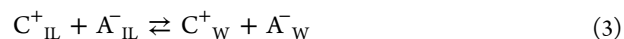
Ion pair extraction:



Ion exchange extraction:



Here, C⁺ and A⁻ denote the IL component cation and anion, respectively; subscripts "W" and "IL" represent the aqueous and IL phases, respectively. In addition, there exists the dissolution equilibrium of IL in the aqueous phase.



The equilibrium constants for eq 1 (ion pair extraction constant, $K_{\text{ex,IP}}$), eq 2 (ion exchange extraction constant, $K_{\text{ex,IE}}$), and eq 3 (solubility product, K_{sp}) are defined as

$$K_{\text{ex,IP}} = [\text{Pic}^-]_{\text{IL}}/[\text{Pic}^-]_{\text{W}}[\text{C}^+]_{\text{W}} \quad (4)$$

$$K_{\text{ex,IE}} = [\text{Pic}^-]_{\text{IL}}[\text{A}^-]_{\text{W}}/[\text{Pic}^-]_{\text{W}} \quad (5)$$

$$K_{\text{sp}} = [\text{C}^+]_{\text{W}}[\text{A}^-]_{\text{W}} \quad (6)$$

Among these equilibrium constants, the following relationship holds.

Table 2. Distribution Ratios and Aqueous Equilibrium Concentrations of Picrate Anion at Different Initial Concentrations of Sodium Picrate at 298.2 K^a

[Pic ⁻] _{w,init} /mmol·dm ⁻³	[Pic ⁻] _w /mmol·dm ⁻³	log D
IL = [HMIIm][PF ₆]		
2.11	0.114	2.238
1.06	0.0564	2.243
0.529	0.0287	2.238
IL = [HMIIm][NTf ₂]		
0.211	0.0578	1.423
0.106	0.0286	1.426
0.0528	0.0144	1.426
IL = [MOIm][PF ₆]		
2.11	0.0374	2.747
1.06	0.0173	2.781
0.529	0.00908	2.760
IL = [MOIm][BETf]		
0.0106	0.00644	0.814
0.00531	0.00332	0.778
0.00266	0.00169	0.754
IL = [BM ₂ Im][NTf ₂]		
1.13	0.768	0.662
0.564	0.386	0.663
0.282	0.192	0.669
IL = [MTOA][NTf ₂]		
2.11	0.431	1.592
1.06	0.0982	1.988
0.528	0.0296	2.225
IL = [BImH][NTf ₂]		
98.3	6.29	1.465
49.0	2.26	1.628
19.6	0.697	1.746
7.85	0.249	1.796
3.89	0.120	1.809
1.97	0.0592	1.820
0.971	0.0294	1.817
0.486	0.0146	1.821
IL = [BPyrH][NTf ₂]		
2.12	0.422	1.601
1.06	0.211	1.608
0.531	0.105	1.606

^aThe volume ratio of the IL phase to the aqueous phase is 1/10.

$$K_{\text{ex,IE}}/K_{\text{ex,IP}} = K_{\text{sp}} \quad (7)$$

The K_{sp} value can be determined as the square of the solubility, assuming the ion activity coefficients to be unity and neglecting any ion association. The values are shown in Table 1.

The aqueous concentrations of C^+ and A^- should be equal to each other when no extraction occurs. Upon the extraction of Pic^- , the aqueous concentration of C^+ decreases (eq 1) and that of A^- increases (eq 2). The difference between the aqueous concentrations of A^- and C^+ corresponds to the decreased amount of the aqueous concentration of Pic^- ($\Delta[\text{Pic}^-]_{\text{w}} = [\text{Pic}^-]_{\text{w,init}} - [\text{Pic}^-]_{\text{w}}$):

$$[A^-]_{\text{w}} - [C^+]_{\text{w}} = \Delta[\text{Pic}^-]_{\text{w}} \quad (8)$$

From eqs 6 and 8, the following equations expressing the aqueous concentrations of C^+ and A^- are derived.

$$[C^+]_{\text{w}} = \{-\Delta[\text{Pic}^-]_{\text{w}} + (\Delta[\text{Pic}^-]_{\text{w}}^2 + 4K_{\text{sp}})^{1/2}\}/2 \quad (9)$$

$$[A^-]_{\text{w}} = \{\Delta[\text{Pic}^-]_{\text{w}} + (\Delta[\text{Pic}^-]_{\text{w}}^2 + 4K_{\text{sp}})^{1/2}\}/2 \quad (10)$$

On the other hand, from eqs 4 and 5, the log D value of Pic^- can be expressed as follows.

$$\log D = \log K_{\text{ex,IP}} + \log[C^+]_{\text{w}} \quad (11)$$

$$\log D = \log K_{\text{ex,IE}} - \log[A^-]_{\text{w}} \quad (12)$$

Substituting $[C^+]_{\text{w}}$ and $[A^-]_{\text{w}}$ in eqs 11 and 12 by eqs 9 and 10, the following equations are obtained.

$$\log D = \log K_{\text{ex,IP}} + \log\{-\Delta[\text{Pic}^-]_{\text{w}} + (\Delta[\text{Pic}^-]_{\text{w}}^2 + 4K_{\text{sp}})^{1/2}\}/2 \quad (13)$$

$$\log D = \log K_{\text{ex,IE}} - \log\{\Delta[\text{Pic}^-]_{\text{w}} + (\Delta[\text{Pic}^-]_{\text{w}}^2 + 4K_{\text{sp}})^{1/2}\}/2 \quad (14)$$

These equations are essentially equal to each other, and it has already been confirmed that they hold for the distribution of Pic^- in some nonprotic IL/water biphasic systems.¹¹ In this study, the applicability of the equations to the distribution of Pic^- in protic IL/water biphasic systems was examined. In Figure 2, the log D value of Pic^- between [BImH][NTf₂] and

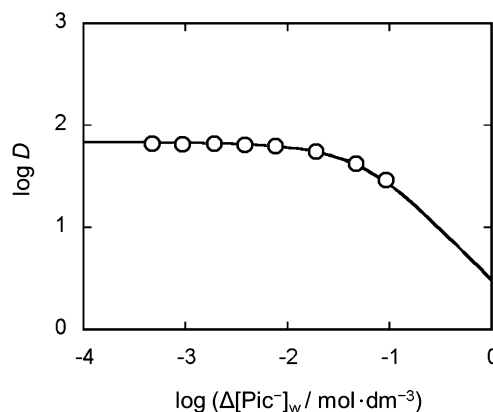


Figure 2. Distribution ratio of picrate anion in the [BImH][NTf₂]/water system as a function of the difference between the initial and equilibrium concentrations of picrate in the aqueous phase. The solid line is the regression curve based on eq 13 or 14.

water is shown as a function of $\Delta[\text{Pic}^-]_{\text{w}}$. A regression curve shown in the figure is generated based on eq 13 or 14 by using the K_{sp} value of [BImH][NTf₂] (Table 1). A good agreement between the experimental results and the regression curve is found (correlation coefficient $r = 0.996$), proving that the distribution in the protic IL/water system is also explained based on the above model.

According to eq 13 or 14, the log D value becomes constant when $\Delta[\text{Pic}^-]_{\text{w}} \ll 2K_{\text{sp}}^{1/2}$ and the log D value in such a dilute condition (log D°) is expressed as follows.

$$\log D^\circ = \log K_{\text{ex,IP}} + \log K_{\text{sp}}^{1/2} \quad (15)$$

$$\log D^\circ = \log K_{\text{ex,IE}} - \log K_{\text{sp}}^{1/2} \quad (16)$$

From the data in Table 2, the $K_{\text{ex,IP}}$ and $K_{\text{ex,IE}}$ values were determined by using eqs 13 and 14, respectively. The D° values were calculated from eq 15 or 16. The logarithmic values of $K_{\text{ex,IP}}$, $K_{\text{ex,IE}}$, and D° are summarized in Table 3.

Table 3. Distribution Ratios of Picrate Anion in Diluted Condition^a and Extraction Equilibrium Constants at 298.2 K

No.	IL	$\log (K_{\text{ex,IP}}/\text{mol}^{-1}\cdot\text{dm}^3)^b$	$\log (K_{\text{ex,IE}}/\text{mol}\cdot\text{dm}^{-3})^b$	$\log D^\circ$
1	[BMIm][PF ₆]	2.709 ^c	0.443 ^c	1.576
2	[BMIm][NTf ₂]	2.64 ^c	-0.93 ^c	0.85
3	[HMIm][PF ₆]	3.848 (0.004)	0.651 (0.004)	2.250
4	[HMIm][NTf ₂]	3.7501 (0.0005)	-0.8920 (0.0005)	1.4290
5	[MOIm][BF ₄]	4.97 ^{c,d}	2.55 ^{c,d}	3.76
6	[MOIm][PF ₆]	4.89 (0.01)	0.70 (0.01)	2.80
7	[MOIm][NTf ₂]	4.73 ^c	-0.83 ^c	1.95
8	[MOIm][BETI]	4.32 (0.02)	-2.75 (0.02)	0.78
9	[BM ₂ Im][NTf ₂]	2.627 (0.001)	-1.290 (0.001)	0.669
10	[BMPyr][NTf ₂]	2.37 ^{c,d}	-1.29 ^{c,d}	0.54
11	[MTOA][NTf ₂]	8.09 (0.05)	-1.10 (0.05)	3.50
12	[BImH][NTf ₂]	3.179 (0.004)	0.488 (0.004)	1.834
13	[BPyrH][NTf ₂]	3.110 (0.002)	0.114 (0.002)	1.612

^aIn the condition that $\Delta[\text{Pic}^-]_{\text{w}} \ll 2 K_{\text{sp}}^{1/2}$. ^bValues in parentheses are standard uncertainties. ^cReference 11. ^dRecalculated in ref 12.

In the ion pair extraction (eq 1), C⁺ is directly concerned with the reaction as a reactant, whereas A⁻ is a component of the solvent. This fact is reflected in the $K_{\text{ex,IP}}$ values: the $K_{\text{ex,IP}}$ value for the [NTf₂]⁻-based or [PF₆]⁻-based IL depends greatly on the kind of C⁺, whereas the values for the ILs having the same C⁺ (e.g., [MOIm]⁺) are generally comparable to each other regardless of the kind of A⁻. In the ion exchange reaction (eq 2), the reverse is true: A⁻ is one of the reactants, whereas C⁺ is a component of the solvent. Indeed, the $K_{\text{ex,IE}}$ values depend largely on the kind of A⁻ but not on the kind of C⁺.

The $K_{\text{ex,IP}}$ value for a given A⁻ decreases in the following C⁺ order: [MTOA]⁺ > [MOIm]⁺ > [HMIm]⁺ > [BImH]⁺ ≈ [BPyrH]⁺ > [BMIm]⁺ ≈ [BM₂Im]⁺ > [BMPyr]⁺. It appears that the ion pair extractability is generally greater with a more hydrophobic C⁺, although there are some exceptional cases such as the protic cations and [BM₂Im]⁺. On the other hand, the $K_{\text{ex,IE}}$ value for a given cation varies with A⁻ in the order, [BF₄]⁻ > [PF₆]⁻ > [NTf₂]⁻ > [BETI]⁻. The ion exchange extractability is greater with a more hydrophilic A⁻.

From the relation of eq 16 and the fact that the $K_{\text{ex,IE}}$ value is insensitive to the kind of C⁺, it is expected that the C⁺ dependence of the D° value is governed by that of the $K_{\text{sp}}^{1/2}$ value, i.e., the aqueous solubility of the IL. In Figure 3, the plots of $\log D^\circ$ versus $\log K_{\text{sp}}^{1/2}$ are shown for the [NTf₂]⁻- and [PF₆]⁻-based ILs with different C⁺. A linear relationship with a slope of -1 is expected from eq 16 and actually observed for each of the following IL groups: the [PF₆]⁻-based ILs with the 1,3-dialkylimidazolium cations (no. 1, 3, and 6), the [NTf₂]⁻-based ILs with the 1,3-dialkylimidazolium cations (no. 2, 4, and 7), and the [NTf₂]⁻-based ILs with [BM₂Im]⁺, [BMPyr]⁺, and [MTOA]⁺ (no. 9, 10, and 11). In the case of the [NTf₂]⁻-based ILs, the line for the 1,3-dialkylimidazolium cations is slightly higher than that for [BM₂Im]⁺, [BMPyr]⁺, and [MTOA]⁺. In addition, the $\log D^\circ$ values for the [NTf₂]⁻-based ILs with the

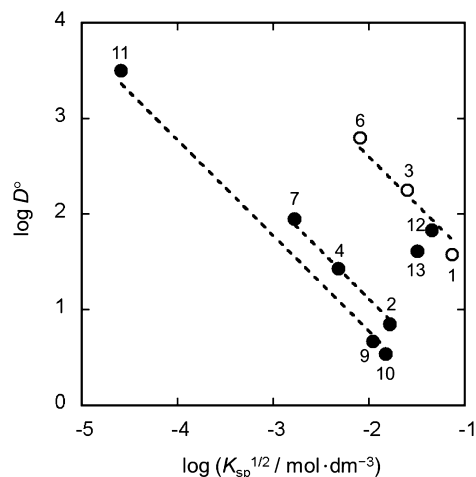


Figure 3. Relationship between $\log D^\circ$ and $\log K_{\text{sp}}^{1/2}$ for [NTf₂]⁻-based ILs (filled circles) and [PF₆]⁻-based ILs (open circles) with different component cations. The numbers of ILs correspond to those in Tables 1 and 3. The broken lines are the regression lines with a slope of -1 for the IL groups [1, 3, 6], [2, 4, 7], and [9, 10, 11].

protic cations (no. 12 and 13) show large upward deviations from the correlation lines for the other [NTf₂]⁻-based ILs. These differences with the type of C⁺ correspond to the magnitude of the $K_{\text{ex,IE}}$ value: the $K_{\text{ex,IE}}$ value is much larger for the protic cations and slightly larger for the 1,3-dialkylimidazolium cations than for [BM₂Im]⁺, [BMPyr]⁺, and [MTOA]⁺. The variation of the ion exchange extractability with the type of C⁺ can be explained in terms of “hydrogen-bond donating ability” or “Lewis acidity” of the IL cations. The protic cation has a positively charged hydrogen atom which should have strong hydrogen bonding with the picrate anion. It is also known that the 1,3-dialkylimidazolium cation has a stronger interaction with the picrate anion through the C2–H atom, as compared to [BM₂Im]⁺ and tetraalkylammonium cations.¹³ Because the cation–anion interaction is stronger for the picrate anion than for the [NTf₂]⁻ anion,¹³ the ion exchange extractability of the picrate anion with the [NTf₂]-based IL increases with an increase of the hydrogen-bond donating ability of the IL cation.

From eq 15, the A⁻ dependence of the D° value is expected to be governed by that of the $K_{\text{sp}}^{1/2}$ value because the $K_{\text{ex,IP}}$ value is insensitive to the kind of A⁻. In Figure 4, the plot of $\log D^\circ$ versus $\log K_{\text{sp}}^{1/2}$ is shown for the [MOIm]⁺-based ILs with different A⁻. A linear relationship with a slope of about 1 (1.3) is observed as expected from eq 15. The slope higher than 1 comes from the slight variation of the $K_{\text{ex,IP}}$ value with A⁻, i.e., [BF₄]⁻ ≥ [PF₆]⁻ ≥ [NTf₂]⁻ > [BETI]⁻. This sequence seems to be consistent with that of the Lewis acidity of the ILs; the values of the Lewis acidity parameter, E_{T}^{N} , are available for the ILs except for [MOIm][BETI], that is, 0.65, 0.633, and 0.627 for [MOIm][BF₄], [MOIm][PF₆], and [MOIm][NTf₂], respectively.²²

CONCLUSION

The solvent effects of ILs on the distribution of an anion in hydrophobic IL/water biphasic systems were studied by using picrate as the distributing anion. The extractability of the anion generally increases with increasing hydrophobicity of the IL cation and increasing hydrophilicity of the IL anion. The dependence of the distribution ratio on the kind of IL cation

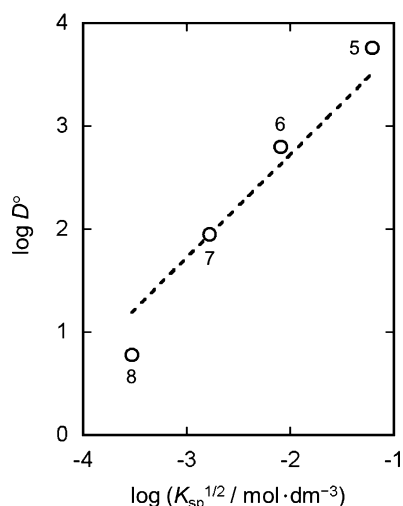


Figure 4. Relationship between $\log D^\circ$ and $\log K_{sp}^{1/2}$ for $[\text{MOIm}]^+$ -based ILs with different component anions. The numbers of ILs correspond to those in Tables 1 and 3. The broken line is the regression line with a slope of 1.

and anion can be quantitatively explained as a function of the solubility of the IL ($K_{sp}^{1/2}$ value). This explanation is based on the model where both the ion pair extraction and the anion exchange extraction proceed. Protic ILs and 1,3-dialkylimidazolium-based ILs are favorable to the anion extraction because the component cations, particularly protic cations, have a strong interaction with the target anion. The regularities found in this study will be utilized for the prediction of the ability of an IL to extract an anion and also for the design of effective extraction systems with ILs.

AUTHOR INFORMATION

Corresponding Author

*E-mail: katsuta@faculty.chiba-u.jp.

Funding

This work was partially supported by a research grant from the Futaba Electronics Memorial Foundation.

Notes

The authors declare no competing financial interest.

REFERENCES

- Huddleston, J. G.; Willauer, H. D.; Swatoski, R. P.; Visser, A. E.; Rogers, R. D. Room Temperature Ionic Liquids as Novel Media for "Clean" Liquid-Liquid Extraction. *Chem. Commun.* **1998**, 1765–1766.
- Visser, A. E.; Swatoski, R. P.; Reichert, W. M.; Willauer, H. D.; Huddleston, J. G.; Rogers, R. D. Room Temperature Ionic Liquids as Replacements for Traditional Organic Solvents and Their Applications towards "Green Chemistry" in Separation Processes. In *Green Industrial Applications of Ionic Liquids*; Rogers, R. D., Seddon, K. R., Volkov, S., Eds.; Kluwer Academic Publishers: Dordrecht, The Netherlands, 2003; pp 137–156.
- Han, X.; Armstrong, D. W. Ionic Liquids in Separation. *Acc. Chem. Res.* **2007**, *40*, 1079–1086.
- Oppermann, S.; Stein, F.; Kragl, U. Ionic Liquids for Two-Phase Systems and Their Application for Purification, Extraction and Biocatalysis. *Appl. Microbiol. Biotechnol.* **2011**, *89*, 493–499.
- Carda-Broch, S.; Berthod, A.; Armstrong, D. W. Solvent Properties of the 1-Butyl-3-methylimidazolium Hexafluorophosphate Ionic Liquid. *Anal. Bioanal. Chem.* **2003**, *375*, 191–199.
- Khachatryan, K. S.; Smirnova, S. V.; Torocheshnikova, I. I.; Shvedene, N. V.; Formanovsky, A. A.; Pletnev, I. V. Solvent Extraction

and Extraction-Voltammetric Determination of Phenols Using Room Temperature Ionic Liquid. *Anal. Bioanal. Chem.* **2005**, *381*, 464–470.

(7) Vijayaraghavan, R.; Vedaraman, N.; Surianarayanan, M.; MacFarlane, D. R. Extraction and Recovery of Azo Dyes into an Ionic Liquid. *Talanta* **2006**, *69*, 1059–1062.

(8) Pei, Y. C.; Wang, J. J.; Xuan, X. P.; Fan, J.; Fan, M. Factors Affecting Ionic Liquids Based Removal of Anionic Dyes from Water. *Environ. Sci. Technol.* **2007**, *41*, 5090–5095.

(9) Li, C.; Xin, B.; Xu, W.; Zhang, Q. Study on the Extraction of Dyes into a Room-Temperature Ionic Liquid and Their Mechanisms. *J. Chem. Technol. Biotechnol.* **2007**, *82*, 196–204.

(10) Katsuta, S.; Nakamura, K.; Kudo, Y.; Takeda, Y.; Kato, H. Partition Behavior of Chlorophenols and Nitrophenols between Hydrophobic Ionic Liquids and Water. *J. Chem. Eng. Data* **2011**, *56*, 4083–4089.

(11) Katsuta, S.; Nakamura, K.; Kudo, Y.; Takeda, Y. Mechanisms and Rules of Anion Partition into Ionic Liquids: Phenolate Ions in Ionic Liquid/Water Biphasic Systems. *J. Phys. Chem. B* **2012**, *116*, 852–859.

(12) Katsuta, S. Distribution Behavior of Neutral and Anionic Compounds in Ionic Liquid/Water Biphasic Systems. *Bunseki Kagaku* **2013**, *62*, 297–315 (in Japanese).

(13) Katsuta, S.; Imai, K.; Kudo, Y.; Takeda, Y.; Seki, H.; Nakakoshi, M. Ion Pair Formation of Alkylimidazolium Ionic Liquids in Dichloromethane. *J. Chem. Eng. Data* **2008**, *53*, 1528–1532.

(14) Katsuta, S.; Yoshimoto, Y.; Okai, M.; Takeda, Y.; Bessho, K. Selective Extraction of Palladium and Platinum from Hydrochloric Acid Solutions by Trioctylammonium-Based Mixed Ionic Liquids. *Ind. Eng. Chem. Res.* **2011**, *50*, 12735–12740.

(15) Freire, M. G.; Neves, C. M. S. S.; Carvalho, P. J.; Gardas, R. L.; Fernandes, A. M.; Marrucho, I. M.; Santos, L. M. N. B. F.; Coutinho, J. A. P. Mutual Solubilities of Water and Hydrophobic Ionic Liquids. *J. Phys. Chem. B* **2007**, *111*, 13082–13089.

(16) Freire, M. G.; Carvalho, P. J.; Gardas, R. L.; Marrucho, I. M.; Santos, L. M. N. B. F.; Coutinho, J. A. P. Mutual Solubilities of Water and the $[\text{C}_n\text{mim}][\text{Tf}_2\text{N}]$ Hydrophobic Ionic Liquids. *J. Phys. Chem. B* **2008**, *112*, 1604–1610.

(17) Anthony, J. L.; Maginn, E. J.; Brennecke, J. F. Solution Thermodynamics of Imidazolium-Based Ionic Liquids and Water. *J. Phys. Chem. B* **2001**, *105*, 10942–10949.

(18) Kakiuchi, T.; Tsujioka, N.; Kurita, S.; Iwami, Y. Phase-Boundary Potential across the Nonpolarized Interface between the Room-Temperature Molten Salt and Water. *Electrochem. Commun.* **2003**, *5*, 159–164.

(19) Alfassi, Z. B.; Huie, R. E.; Milman, B. L.; Neta, P. Electrospray Ionization Mass Spectrometry of Ionic Liquids and Determination of Their Solubility in Water. *Anal. Bioanal. Chem.* **2003**, *377*, 159–164.

(20) Pereiro, A. B.; Rodríguez, A. Experimental Liquid-Liquid Equilibria of 1-Alkyl-3-methylimidazolium Hexafluorophosphate with 1-Alcohols. *J. Chem. Eng. Data* **2007**, *52*, 1408–1412.

(21) Kato, R.; Gmehling, J. Systems with Ionic Liquids: Measurement of VLE and γ^∞ Data and Prediction of Their Thermodynamic Behavior Using Original UNIFAC, mod. UNIFAC(Do), and COSMO-RS(OI). *J. Chem. Thermodynamics* **2005**, *37*, 603–619.

(22) Jessop, P. G.; Jessop, D. A.; Fu, D.; Phan, L. Solvatochromic Parameters of Solvents of Interest in Green Chemistry. *Green Chem.* **2012**, *14*, 1245–1259.